

CFD METHOD FOR ANALYSIS OF THE EFFECT OF DRILL PIPE ORBITAL MOTION SPEED AND ECCENTRICITY ON THE VELOCITY PROFILES AND PRESSURE DROP OF DRILLING FLUID IN LAMINAR REGIME

Hicham Ferroudji^{1*}, Ahmed Hadjadji¹, Titus Ntow Ofei², Mohammad Aziz Rahman³, Ibrahim Hassan⁴ and Ahmed Haddad⁵

¹ Laboratory of Petroleum Equipment's Reliability and Materials, Hydrocarbons and Chemistry Faculty, Université M'Hamed Bougara, Boumerdes, Algeria

² Department of Geoscience and Petroleum Norwegian University of Science & Technology S.P. Andersens veg 15a, 7031 Trondheim, Norway

³ Department of Petroleum Engineering, Texas A&M University at Qatar, Qatar

⁴ Department of Mechanical Engineering, Texas A&M University at Qatar, Qatar

⁵ Research Centre in Industrial Technologies CRTI. BP 64, route de Dely-Ibrahim, Chéraga, Algiers, 16033 Algeria

Received July 4, 2019; Accepted October 8, 2019

Abstract

Due to the axial and lateral loads applied to the drill pipe during the drilling process, this last may lose its stability and begins to make complicated motions like the orbital one. In the present paper, this orbital motion of the drill pipe is modelled using CFD method to investigate its effect on the axial and tangential velocity profiles in the wide and narrow regions of the eccentric annulus ($E=0.2$, $E=0.4$, $E=0.6$ and $E=0.8$), as well as, effect of the orbital motion speed on pressure drop gradient of drilling fluid is studied. Our results show that increment of the orbital motion speed from 100 to 400 rpm causes an increase of 913% of the maximum axial velocity, however, this increment is estimated at about 100% in the case where the drill pipe makes pure rotation for the eccentric annulus ($E=0.8$). Moreover, orbital motion of the inner pipe prevents the secondary flow to appear in the wide region of eccentric annulus. For all eccentricities, the tangential velocity of the orbital motion case in the narrow region for 400 rpm speed is 120% higher than pure rotation one.

Keywords: Orbital motion; eccentricity; velocity profiles; pressure drop; drilling fluid; laminar flow.

1. Introduction

The main role of the drill pipe is to transmit torque from the top drive to the bit where the drill pipe is under axial and lateral loads, which result in axial, lateral and torsional vibrations. Due to these vibrations, drill pipe may lose its stability and begin to make very complicated motions such as orbital motion [1].

Nouri *et al.* [2] experimentally studied the flow of Newtonian and non-Newtonian (power-law) fluids in concentric and eccentric annulus. Their results show that the flow resistance of power-law fluid was decreased by 22.5% when the eccentricity increases from zero to unity. Based on the experimental study, Nouri and Whitelaw [3] found that rotation of the inner pipe makes the axial velocity profile of power-law fluid flatter with a maximum of the axial velocity 5% smaller than the situation without rotation for concentric annulus. Then, Nouri and Whitelaw [4] extended their experimental study to the eccentric annulus. They stated the appearance of a secondary flow (counter rotating swirl) in the wide region of eccentric annulus.

Meuric *et al.* [5] used the finite volume method (FVM) to solve the continuity and momentum equations for yield power-law model flowing through concentric and eccentric annulus in laminar regime. Results indicated that volumetric flowrate decreases with the inner pipe rotation

for eccentric annulus, contrary to the concentric case where volumetric flowrate increases with the inner pipe rotation.

Neto *et al.* [6] used a CFD approach to study non-Newtonian fluid flow through concentric and eccentric annulus. It was found that the axial velocity in the narrow region of the eccentric annulus is significantly smaller than the axial velocity in the wide region of eccentric annulus. Nevertheless, the rotation of the inner pipe is found to increase the axial velocity in the narrow region of eccentric annulus, which enhances the cleaning process during drilling operation. The same conclusion was made by Ofei *et al.* [7] to yield power-law flow fluid.

Vieira Neto *et al.* [8] carried out a numerical study about the influence of the inner pipe rotation on the axial and tangential velocity distribution of power law fluid in concentric and eccentric annulus. Moreover, effect of the inner pipe rotation on pressure drop is evaluated. To validate their numerical study, authors conducted an experimental study using flow loop. It was stated that the increase of the inner pipe rotation causes a decrease of pressure drop for concentric annulus in contrast to the eccentric annulus, where they found that pressure drop increases with the inner pipe rotation.

Bicalho *et al.* [9] also used the CFD technique to investigate the flow of yield power-law in an obstructed section of concentric and eccentric annulus with orbital motion of the inner pipe. An experimental setup was established to validate their numerical results. They found that orbital motion of the inner pipe causes an increment of the tangential velocity in the vicinity of the inner pipe. However, authors did not consider orbital motion of the inner pipe in their study.

Most of the previous studies of non-Newtonian fluids flowing through annular section did not take into account orbital motion of the inner pipe, and authors considered that the inner pipe makes only pure rotation around its own axis [10-13]. Till now, there are limited studies in the literature about effect of the orbital motion on distribution of the axial and tangential velocity profiles of non-Newtonian fluids flowing through eccentric annulus. In the present paper, the effect of the orbital motion speed and eccentricity on distribution of the axial and tangential velocity profiles and pressure drop gradient of power-law fluid are evaluated using CFD commercial software (ANSYS Fluent 16.0) and then the velocity profiles are compared to the case where the inner pipe makes pure rotation.

2. Materials and methods

2.1. Physical model

The domain flow of non-Newtonian fluid (power-law) is bounded by two cylinders where the outer pipe (casing) is fixed, and the inner pipe (drill pipe) makes orbital motion around its own central axis to simulate the drilling fluid pattern in the borehole.

When the inner pipe rotation reaches 80 to 110 rpm around its own central axis, the inner pipe begins to make an orbital motion around the center of the outer pipe [14]. For that, in the present study, the orbital motion speed is considered to increase (from 0 to 400 rpm) with increasing of the inner pipe rotation (from 0 to 400 rpm) simultaneously.

2.2. Mathematical equations

The flow of non-Newtonian fluid (power-law) through eccentric annulus where the inner pipe makes an orbital motion is considered to be fully developed, incompressible, steady and isothermal in laminar regime.

The continuity and momentum equations that govern the flow can be listed as follows:

$$\frac{\partial U_i}{\partial x_i} = 0 \quad (1)$$

$$U_j \frac{\partial U_i}{\partial x_j} = -\frac{1}{\rho} \frac{\partial P}{\partial x_i} + \frac{\partial}{\partial x_j} \left(\frac{\mu}{\rho} \frac{\partial U_i}{\partial x_j} - \tau_{ij} \right) + S_i \quad (2)$$

where x_i are the coordinate axes (x, y , and z); U_i are components of the velocity vector; P is the pressure; ρ is the density; μ is the fluid viscosity; τ_{ij} are components of the Reynolds stress tensor and S_i is the sum of body forces.

The rheological model considered in this study is the power-law as follows:

$$\tau = K(\dot{\gamma})^n \tag{3}$$

where K is the flow consistency index, and n is the flow behavior index.

The rheological parameters of the power-law fluid are given in Table 1 as follows:

Table 1. Fluid and geometry characteristics.

Rheological behavior	Fluid and geometry characteristics			
	K [Pa.s ⁿ]	n [-]	Do [mm]	Di [mm]
Non-Newtonian (power-law)	0.93	0.52	38.1	19.05

The eccentricity of the outer and inner cylinders is characterized by the following relationship:

$$E = \frac{2.e}{(D_o - D_i)} \tag{4}$$

where e is the distance between the inner and outer cylinders.

2.3. Simulation method

The annular space is subdivided into 1.2×10^6 and 1.76×10^6 elements for annulus where the inner pipe makes the pure rotation and orbital motion, respectively. The number of elements is selected to ensure that the obtained results are independent of the mesh models adopted as well as keeping the number of elements as low as possible to optimize computational time, as shown in Fig. 1a. The mesh is refined near walls to capture high variation of calculated solutions in these regions. Since the inner pipe makes both orbital motion and pure rotation at the same time, moving mesh technique is used to describe this kind of motion. For that, the annular flow domain is divided into 3 parts: inner part (partly influenced by pure rotation of the inner pipe), middle part (partly influenced by orbital motion of the inner pipe), and outer part (stationary part) as seen in the Fig. 1b. The orbital motion in the present work is obtained by rotation of the inner part around the axis of the inner pipe and rotation of the middle part around the axis of the outer pipe. Therefore, Angular velocity of the inner and middle parts is the orbital motion speed. Thus, the three parts of the domain flow are related to two interfaces (interface1 and interface2), which allow to transfer pressure, velocity, and other variables.

The commercial code ANSYS Fluent 16.0 based on the finite volume method is used to solve the differential equations, where the flow equations are integrated over each control volume. All simulations of the present numerical study were run in the unsteady state due to the moving mesh where the position of the inner pipe is updated according to the orbital motion speed every time step. All simulation runs were carried out in laminar regime. SIMPLE algorithm is employed for coupling pressure-velocity, and PRESTO scheme is used for discretization of pressure. For discretization of the momentum equation first-order upwind is used to overcome instabilities and convergence problems that can induced by high-order discretization in the presence of moving mesh. As a convergence criteria, 10^{-5} is selected for all simulations.

2.4. Validation model

Due to the limited experimental data in the literature about non-Newtonian fluids flowing through annular space where the inner pipe makes an orbital motion, the CFD model used in the present study is validated using the experimental work of [4] where mesh of the inner part rotates around the center of the inner pipe which produces pure rotation, while mesh of the middle and outer parts of the domain flow are kept stationary. Fig. 1c depicts that the numerical results are in good concordance with the experimental data where the mean error of the tangential velocity is 12%; however, for the axial velocity, the mean error is estimated at around 14.3% and 8.4% for 0 rpm and 300 rpm, respectively.

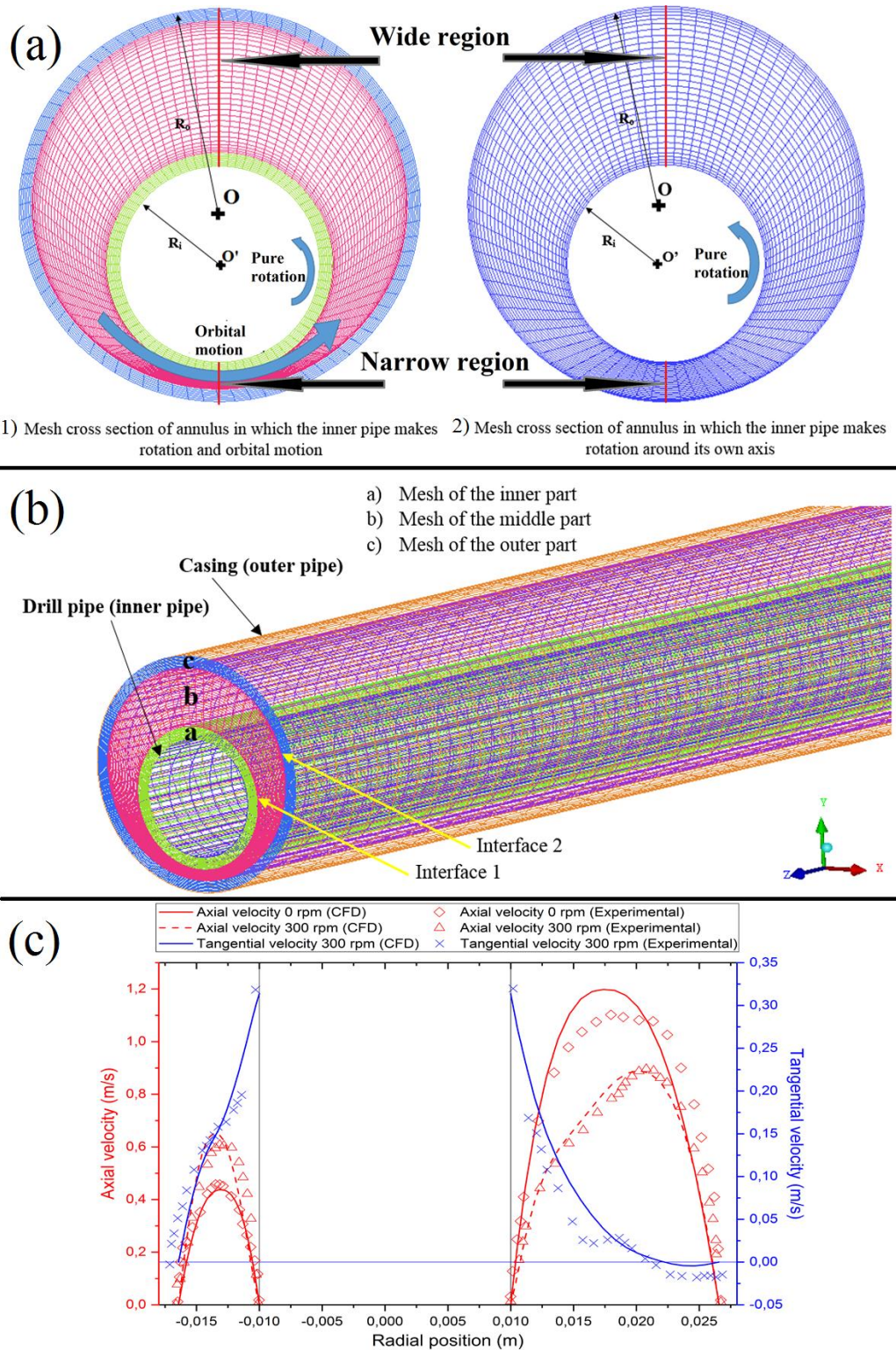


Fig. 1. a. Cross section of the mesh and lines where the velocity profiles are obtained. b. Flow domain of the power-law fluid. b. Comparison of the numerical results with the experimental data [4]

3. Results and discussion

3.1. Axial velocity

Fig. 2a presents the axial velocity profile of power-law fluid in the laminar regime for eccentric the annulus ($E = 0.2$). As it can be seen, both pure rotation and orbital motion cause an increase of the axial velocity maximums in the narrow region of the annulus where presence of the orbital motion causes an additional increase for all cases especially for 100 rpm in which the increase is around 23% compared with the situation where the inner pipe makes pure rotation. This effect is beneficial for transporting cuttings and prevent formation of cuttings bed in horizontal wells. On the other hand, the axial velocity in the wide region diminishes with increase of the orbital motion speed for both orbital motion and pure rotation cases.

As shown in Fig. 3a, The calculated axial velocity profiles of the eccentric annulus ($E = 0.4$) in the narrow region indicate that orbital motion of the inner pipe has a significant effect on the axial velocity of the power-law fluid compared to the pure rotation case where the axial velocity maximum of the orbital motion case is 59% greater than pure rotation one for 200 rpm and 300 rpm speeds. This increase could contribute to the hole cleaning process by removing the deposited cuttings on the lower side of annulus. The widest region of the annulus shows a decrease of the axial velocity gradient near the inner pipe when the orbital motion speed reaches 300 rpm which could be considered as an indication for a reverse flow (in the opposite direction of the main axial flow) in this region when eccentricity exceeds ($E = 0.4$) value.

Fig. 4a shows that an increase of pure rotation speed from 100 to 400 rpm induces an increase of 304% of the axial velocity maximum in the narrow region of the eccentric annulus ($E = 0.6$); however this increase is estimated at around 551% for orbital motion situation. Moreover, comparison of the axial velocity profile of orbital motion case with that of pure rotation for 400 rpm speed shows that the axial velocity maximum of orbital motion case is 173% higher than pure rotation one which proves that appearance of the orbital motion would significantly enhance the hole cleaning process especially in horizontal and deviated wells. For the wide region of the annulus, a stagnation region of the power-law fluid near the inner pipe is observed when the orbital motion speed reaches 400 rpm. This phenomenon could be attributed to beginning formation of the reverse flow in this region.

In Fig. 5a, pure rotation of the inner pipe has a slight effect on the axial velocity profile for both narrow and wide regions of the eccentric annulus ($E = 0.8$). In contrast to the orbital motion case where increase of the orbital motion speed from 100 to 400 rpm causes an increment of 912% of the axial velocity maximum in the narrow region of the eccentric annulus. The wide region shows that increase of the orbital motion speed causes a decrease of the axial velocity gradient near the inner pipe until 300 rpm where a reverse flow is observed. The reverse flow in the opposite direction of the main flow is caused by orbital motion of the inner pipe in which the maximum value in this reverse flow is 1.4% and 12.8% of the bulk axial velocity for 300 rpm and 400 rpm, respectively. The appearance of such kind of reverse flow could increase shear stress near the inner pipe resulting in increment of pressure drop of flowing fluid.

3.2. Tangential velocity

Fig. 2b outlines the distribution of the tangential velocity profile for eccentric annulus ($E = 0.2$). Increase of the pure rotation and the orbital motion speed from 100 to 400 rpm induce an increase of 300% of the tangential velocity near the inner pipe in the narrow region for both cases (pure rotation and orbital motion). A comparison of the tangential velocity in this region for 400 rpm speed indicates that orbital motion case is 120% higher than pure rotation case. This would improve the erosion effect of the cuttings bed by the inner pipe to get transported in the main flow, which improves the cleaning process of the well. Almost, a similar effect is observed for the wide region near the inner pipe. Moreover, it is worthy to note that the orbital motion causes a considerable increase in the tangential velocity in the middle of the wide region.

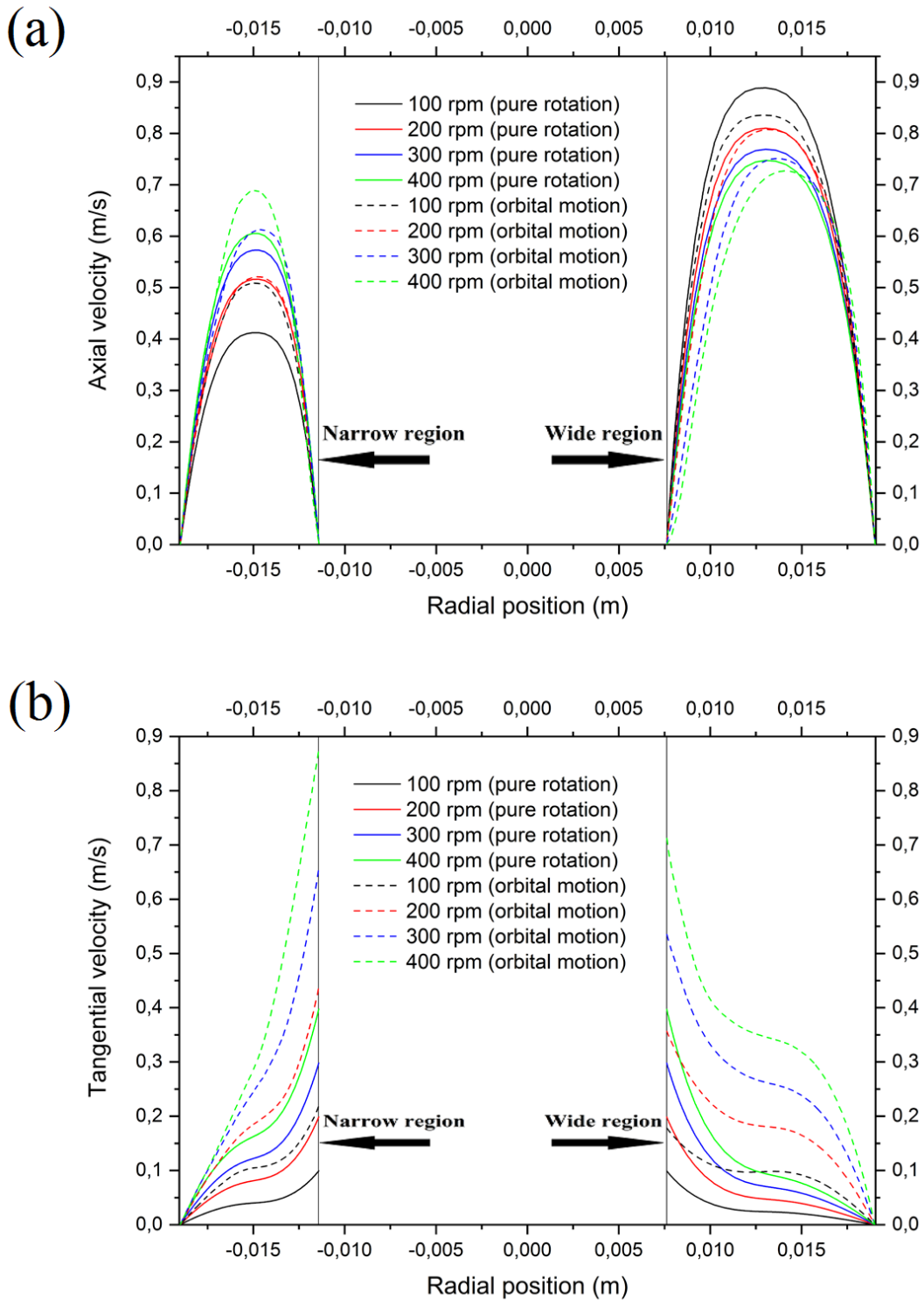


Fig. 2. a. Axial velocity profiles for various pure rotation and orbital motion speeds ($E = 0.2$)
 b. Tangential velocity profiles for various pure rotation and orbital motion speeds ($E = 0.2$)

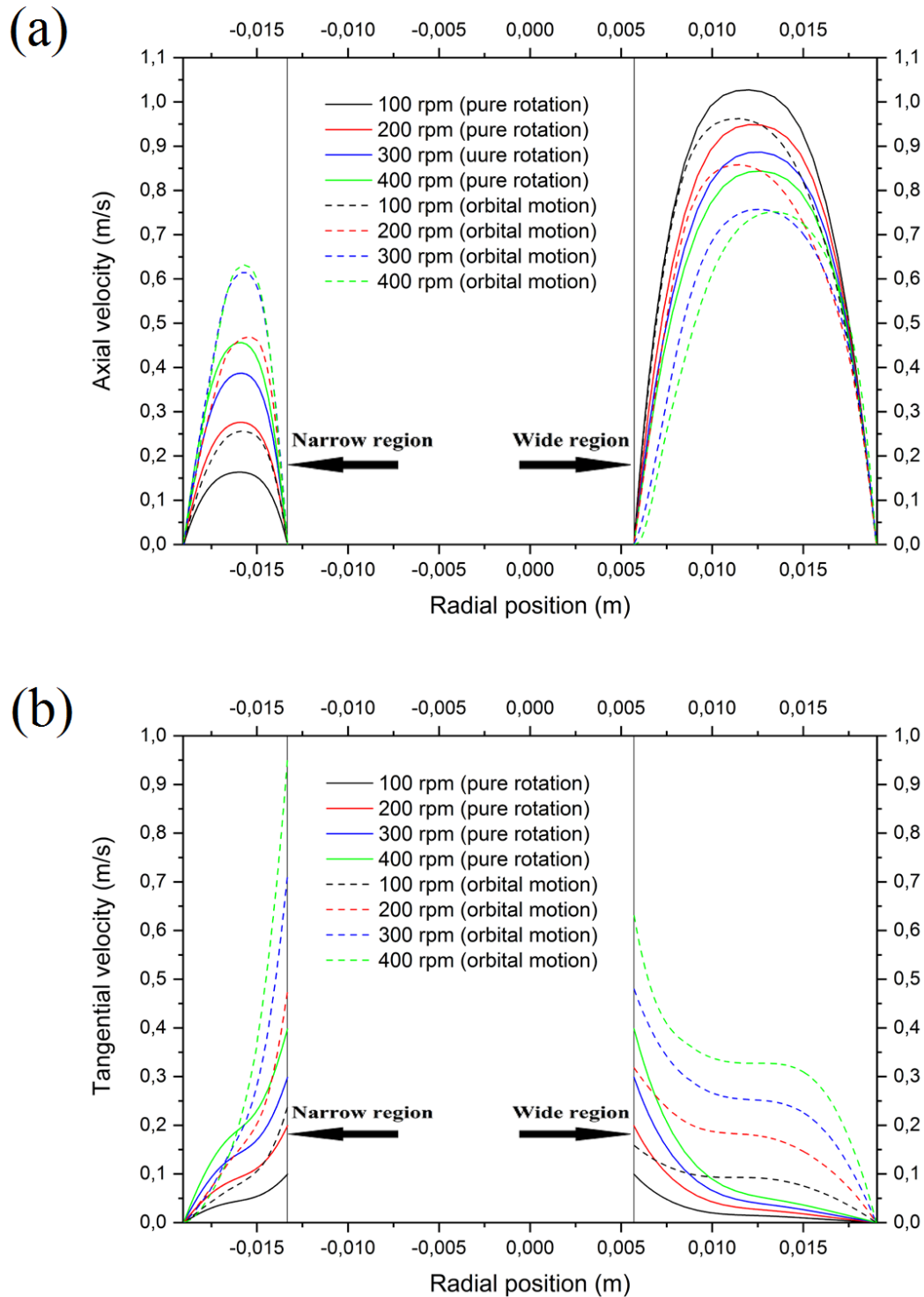


Fig. 3.a. Axial velocity profiles for various pure rotation and orbital motion speeds ($E=0.4$).
 b. Tangential velocity for various pure rotation and orbital motion speeds ($E=0.4$)

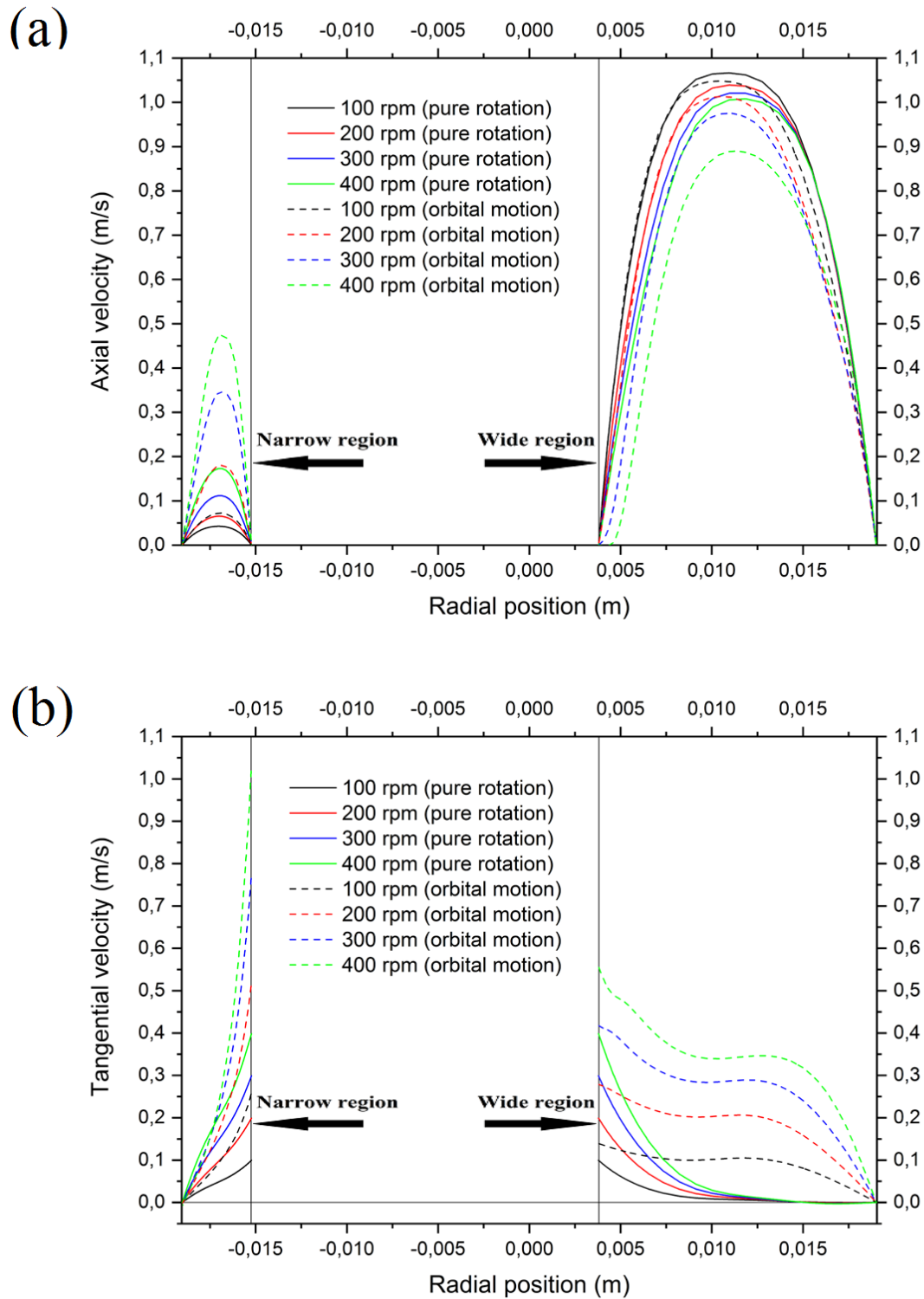


Fig. 4.a. Axial velocity profiles for various pure rotation and orbital motion speeds ($E=0.6$).
 b. Tangential velocity for various pure rotation and orbital motion speeds ($E=0.6$)

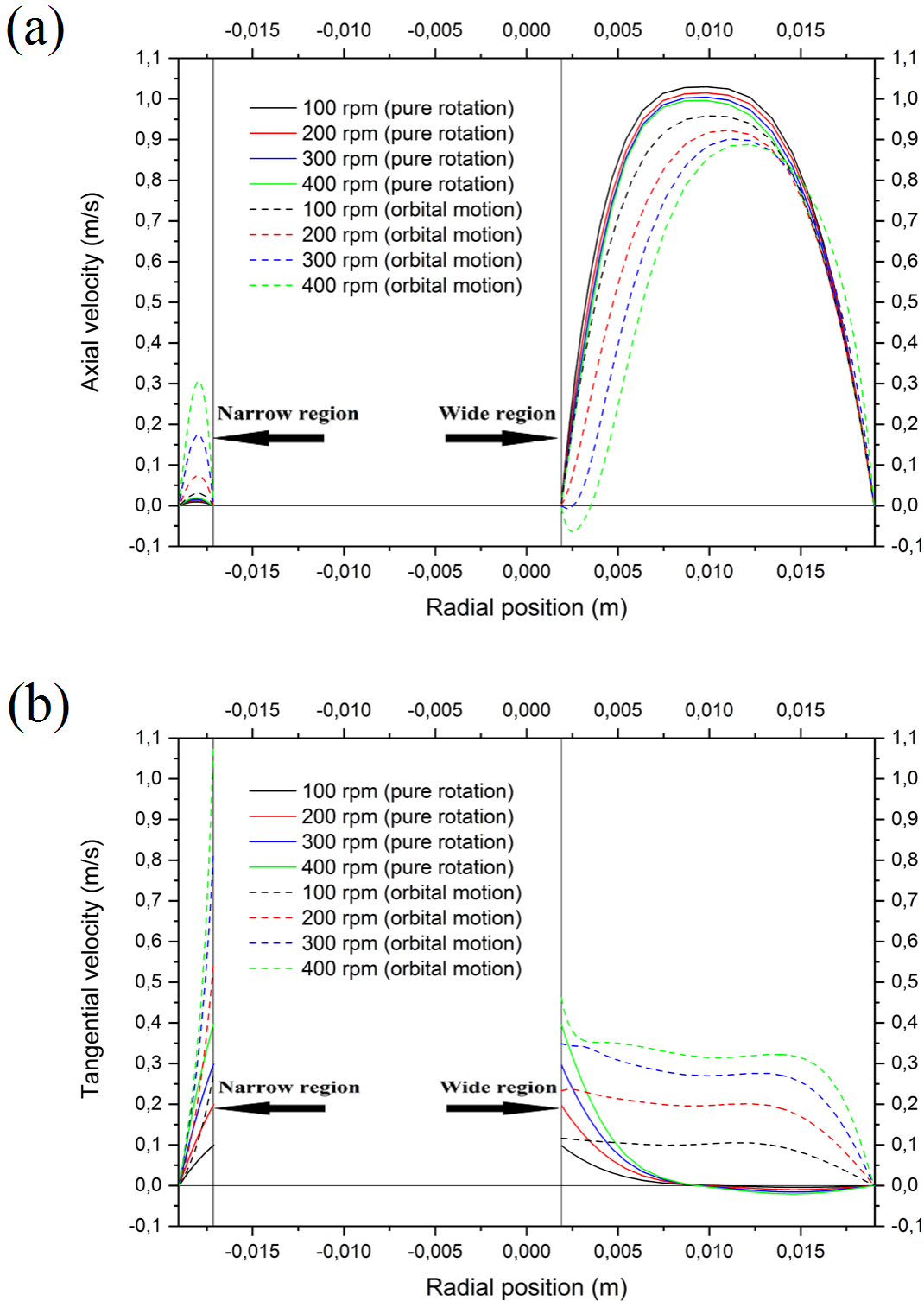


Fig. 5.a. Axial velocity profiles for various pure rotation and orbital motion speeds ($E=0.8$).
 b. Tangential velocity for various pure rotation and orbital motion speeds ($E=0.8$)

Fig. 3b indicates that the tangential velocity of power-law fluid around the inner pipe increases with the increase of pure rotation speed for both narrow and wide regions of the eccentric annulus ($E = 0.4$). The tangential velocity near the inner pipe is found to increase

with orbital motion speed where this effect is more pronounced in the narrow region of the eccentric annulus for all orbital motion speeds. Furthermore, a considerable increase of the tangential velocity in the middle of the wide region induced by orbital motion compared to the increase caused by pure rotation of the inner pipe.

Fig. 4b shows the distribution of the tangential velocity in the eccentric annulus ($E = 0.6$), where a secondary flow (also called counter-rotating swirl) begins to appear near the outer pipe of the wide region contrary to the orbital motion case where the tangential velocity increases with orbital motion speed.

As shown in Fig. 5b, a fully developed secondary flow is observed in the wide region of the eccentric annulus ($E = 0.8$) in which its form gets larger with increase of pure rotation of the inner pipe. The orbital motion of the inner pipe prevents such kind of secondary flows to appear where the power-law fluid rotates in the same direction of the inner pipe.

3.3. Pressure drop gradient

As can be seen in Fig. 6, for an eccentricity equal to ($E = 0.2$), an increase of the pure rotation speed of the inner pipe has a slight effect on pressure drop gradient; however, for the orbital motion case, pressure drop is decreased. This effect could be attributed to enhancement of the shear thinning effect by orbital motion of the inner pipe for this eccentric annulus. Pressure drop gradient increases with increase of the pure rotation and orbital motion speed from 100 to 400 rpm for the eccentric annulus ($E = 0.4$, $E = 0.6$ and $E = 0.8$) where pressure drop is more increased when the inner pipe makes an orbital motion. This behavior indicates that inertial effects dominate the shear thinning phenomenon for these eccentricities.

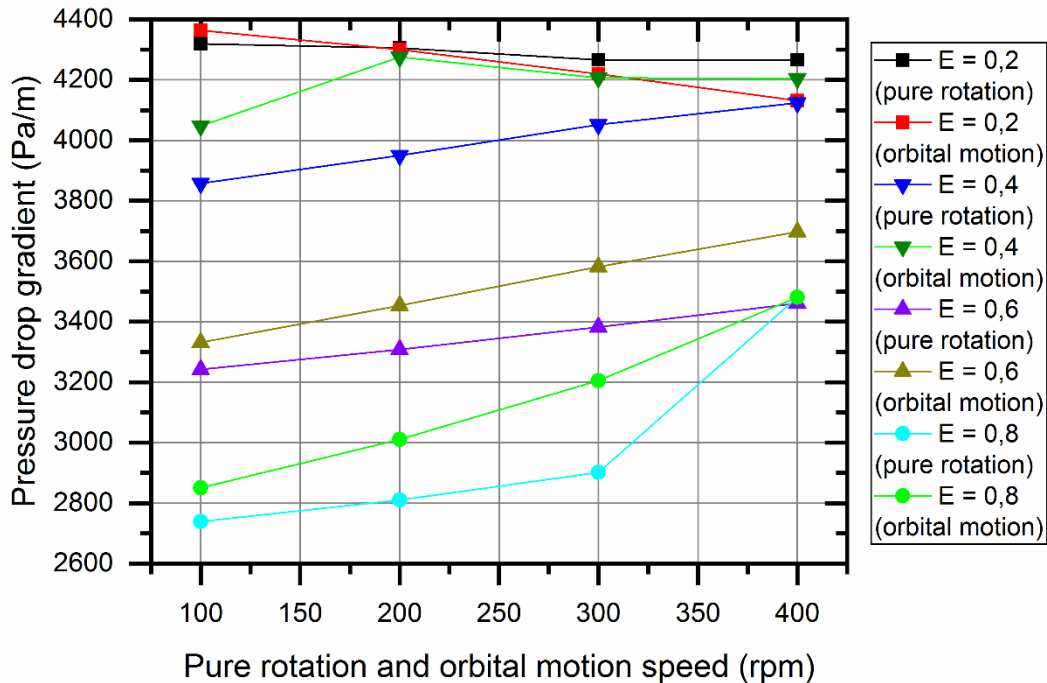


Fig. 6. Effect of the orbital motion and pure rotation of the inner pipe on pressure drop gradient of the power-law fluid for various eccentricities

4. Conclusions

In this paper, moving mesh is used to simulate the flow of power-law fluid flowing through eccentric annulus in laminar regime in which the inner pipe makes pure rotation and orbital motion. Numerical results highlight effect of the orbital motion for various eccentricities on distribution of the axial and tangential velocity profiles in the annular section, as well as its effect on pressure drop. The following can be concluded from this numerical investigation:

- As eccentricity increases, pure rotation effect of the inner pipe on the axial velocity in the narrow region of eccentric annulus diminishes till ($E = 0.8$) where the effect becomes negligible, however, for the orbital motion case, increase of the orbital motion speed from 100 to 400 rpm causes an increase of 912% of the axial velocity maximum which would enhance cleaning process in the deviated and horizontal wells.
- When the orbital motion speed reaches 300 rpm, a reverse flow near the inner pipe in the wide region of the eccentric annulus ($E = 0.8$) is observed. This effect is not stated for pure rotation case.
- Pure rotation causes the appearance of secondary flow in the wide region of eccentric annulus when the eccentricity reaches ($E = 0.6$). While orbital motion of the inner pipe prevents appearance of the secondary flow where the flow of power-law fluid is rotating in the direction of the inner pipe
- Increase of the pure rotation and the orbital motion speed from 100 to 400 rpm induce an increase of 300% of the tangential velocity near the inner pipe in the narrow region of annulus for both cases (pure rotation and orbital motion) where the tangential velocity in this region for 400 rpm speed is 120% higher than pure rotation case. This effect is almost similar for all eccentricities. This would improve the erosion effect of the cuttings bed by the inner pipe to get transported in the main flow, which improves the cleaning process of the well.
- The orbital motion of the inner pipe enhances shear thinning effect which induces a decrease of pressure drop gradient with increase of the orbital motion speed for the eccentric annulus ($E = 0.2$). For other eccentricities ($E = 0.4$, $E = 0.6$, and $E = 0.8$), increment of the orbital motion speed, causes an increase of pressure drop.

Acknowledgement

This publication was also made possible by the grant NPRP10-0101-170091 from Qatar National Research Fund (a member of the Qatar Foundation). Statements made herein are solely the responsibility of the authors.

Nomenclature

D_o	diameter of the outer cylinder (m)	n	flow behavior index (-)
D_i	diameter of the inner cylinder (m)	u	bulk flow velocity (m/s)
E	eccentricity of the inner cylinder (-)	ρ	fluid density (kg/m^3)
K	flow consistency index ($\text{Pa}\cdot\text{s}^n$)	$\dot{\gamma}$	shear rate (s^{-1})

References

- [1] Gao G, Miska S. SPE J., 2010; 15: 867-877.
- [2] Nouri JM, Umur H, Whitelaw JH. J. Fluid Mech., 1993; 253: 617-641.
- [3] Nouri JM, Whitelaw JH. J. Fluids Eng., 1994; 116: 821-827.
- [4] Nouri JM, Whitelaw JH. Int. J. Heat Fluid Flow, 1997; 18: 236-246.
- [5] Meuric OF, Wakeman RJ, Chiu TW, Fisher KA. Can. J. Chem. Eng., 1998; 76: 27-40.
- [6] Neto JV, Martins AL, Neto AS, Ataíde CH, Barrozo MAS. Can. J. Chem. Eng., 2011; 89: 636-646.
- [7] Ofei TN, Irawan S, Pao W, Osgouei RE. Can. J. Chem. Eng., 2015; 93: 150-165.
- [8] Vieira Neto JL, Martins AL, Ataíde CH, Barrozo MAS. Braz. J. Chem. Eng., 2014; 31: 829-838.
- [9] Bicalho IC, Mognon JL, Ataíde CH, Duarte CR. Can. J. Chem. Eng., 2016; 94: 391-401.
- [10] Ofei TN, Irawan S, Pao W J. Pet. Eng., 2014; Article ID 486423, doi:10.1155/2014/48642.
- [11] Ozbayoglu EM, Sorgun M. J. Can. Pet. Technol., 2010; 49: 57-64.
- [12] Sultan RA, Rahman MA, Rushd S, Zendejboudi S, Kelessidis VC. Particulate Science and Technology, 2018; 1-13.
- [13] Zahid AA, ur Rehman SR, Rushd S, Hasan A, Rahman MA. Frontiers in Energy (2018) 1-9, <https://doi.org/10.1007/s11708-018-0582-y>.
- [14] Avila RJ, Pereira EJ, Miska SZ, Takach NE. SPE Drill. Complet., 2008; 23: 132-141.

To whom correspondence should be addressed: Dr. Hicham Ferroudji, Laboratory of Petroleum Equipment's Reliability and Materials, Hydrocarbons and Chemistry Faculty, Université M'Hamed Bougara, Boumerdes, Algeria, E-mail hichamf32@gmail.com, ferroudji.h@univ-boumerdes.dz